photonics

Article

Nonreciprocity Steered with a Spinning Resonator

Xiao Shang [1,2,3], Hong Xie [4], Gongwei Lin [1,2,3] and Xiumin Lin [1,2,3,*]

[1] Fujian Provincial Key Laboratory of Quantum Manipulation and New Energy Materials, College of Physics and Energy, Fujian Normal University, Fuzhou 350117, China
[2] Fujian Provincial Engineering Technology Research Center of Solar Energy Conversion and Energy Storage, Fuzhou 350117, China
[3] Fujian Provincial Collaborative Innovation Center for Advanced High-Field Superconducting Materials and Engineering, Fuzhou 350117, China
[4] Department of Mathematics and Physics, Fujian Jiangxia University, Fuzhou 350108, China
* Correspondence: xmlin@fjnu.edu.cn

Abstract: An approach is presented to study the controllable nonreciprocal transmission in a spinning resonator. It has been demonstrated in optomechanics that an optical signal field can only be affected when it propagates in the same direction as the driving field. We show that such an optomechanically induced nonreciprocity can be controlled by rotating the resonator, which introduces a frequency shift with different signs for clockwise and counterclockwise optical fields in the resonator. In our scheme, the transmission probabilities of the clockwise and counterclockwise input signal fields can be reversed by tuning the rotation velocity of the resonator. By studying the transmission spectra of the signal field, we also reveal that the nonreciprocity response can be realized in the spinning resonators in the absence of optomechanical coupling, which extends its utility.

Keywords: optomechanics; nonreciprocity; spinning resonators

Citation: Shang, X.; Xie, H.; Lin, G.; Lin, X. Nonreciprocity Steered with a Spinning Resonator. *Photonics* **2022**, *9*, 585. https://doi.org/10.3390/photonics9080585

Received: 25 July 2022
Accepted: 17 August 2022
Published: 18 August 2022

1. Introduction

Nonreciprocity is considered to be the property of a system in which a beam of light and its reverse light exhibit different optical characteristics in terms of reflection, refraction, and absorption [1]. In other words, the bidirectional symmetry of electromagnetic wave propagation is effectively broken, which makes nonreciprocity become a new key element for signal routing and optical isolation devices in unconventional ways [2,3]. With the continuous development of quantum technology, there is expected to be more demand for nonreciprocal components in future optical data processing.

Optical nonreciprocal transmission has attracted a great deal of interest in the recent past. It has been theoretically investigated and experimentally demonstrated by exploiting spatiotemporal modulations [4–7], synthetic magnetism [8–10], optomechanical interactions [11–23], parity-time symmetric structures [24–27], nonlinear components [28,29], interacting with atoms [30–33], phonon-mediated methods [34,35], and quantum squeezing [36]. These solutions play an important role in various realizations of quantum technology. It is worth noting that spinning resonators may open up a new alternative way to achieve nonreciprocal transmission [37,38] by utilizing the Sagnac effect, which leads to the light circulating in the resonator experiencing an opposite Sagnac–Fizeau shift [39]. Subsequently, several nonreciprocal phenomena related to the Sagnac effect have been deeply explored in spinning resonators, including optical nonreciprocity [40–43], nonreciprocal photon blockade [38,44–48], nonreciprocal phonon blockade [49], nonreciprocal phonon laser [50–52], nonreciprocal magnon laser [53], nonreciprocal quantum entanglement [54–56], and nonreciprocal chaos [57].

In this paper, we study the nonreciprocal transmission that can be steered with a rotating resonator. When the resonator is rotated, the degenerate clockwise and counterclockwise whispering gallery modes gain frequency shifts with different signs [39], and the

symmetry of the two modes is broken. It is known that the optomechanical interaction in a whispering gallery resonator can be only enhanced in the direction from which the driving field comes [58]. Thus, a signal field is only affected by the optomechanical coupling when it propagates in the same direction as the driving field. This also implies that the system exhibits nonreciprocal behavior [11]. We show that the optomechanically induced nonreciprocity is adjustable by tuning the rotation velocity of the resonator according to the frequency shifts of the two modes. The transmission probabilities of the clockwise and counterclockwise input fields can be reversed if the frequency shift is greater than the cavity linewidth. Our scheme is feasible with current experimental parameters.

The paper is organized as follows. The considered optomechanical system is described and its full Hamiltonian is effectively approximated in Section 2. By evaluating the transmission probability in the frequency domain, the controllable nonreciprocity is investigated with and without optomechanical coupling in Section 3. Finally, a brief discussion and conclusion are given in Section 4.

2. Model

Consider an optomechanical system in a spinning optical resonator, which is side-coupled to a waveguide as illustrated in Figure 1, with optical resonance frequency ω_c and mechanical oscillation frequency ω_m. The Hamiltonian of the system reads ($\hbar = 1$)

$$\begin{aligned} H = {} & (\omega_c + \Delta_F) a_{cw}^\dagger a_{cw} + (\omega_c - \Delta_F) a_{ccw}^\dagger a_{ccw} + \omega_m b^\dagger b \\ & - g(b + b^\dagger)(a_{cw}^\dagger a_{cw} + a_{ccw}^\dagger a_{ccw}) \\ & + \alpha_L (a_{ccw} e^{i\omega_L t} + a_{ccw}^\dagger e^{-i\omega_L t}), \end{aligned} \tag{1}$$

where $a_{cw/ccw}$ and b refer to the photon and phonon annihilation operators for the cavity mode and the mechanical oscillator, respectively, g signifies the optomechanical coupling strength, α_L represents the driving field strength with frequency ω_L. The rotation of the resonator introduces a Fizeau shift [37,39,59]

$$\Delta_F = \frac{n_r r \Omega \omega_c}{c} \left(1 - \frac{1}{n_r^2} - \frac{\lambda}{n_r} \frac{dn_r}{d\lambda} \right). \tag{2}$$

Here, n_r (r) expresses the refractive index (radius) of the resonator and c (λ) denotes the speed (wavelength) of light in vacuum. Note that the Fizeau shift Δ_F has the same sign as the rotation velocity Ω, which is positive (negative) when the resonator rotates counterclockwise (clockwise).

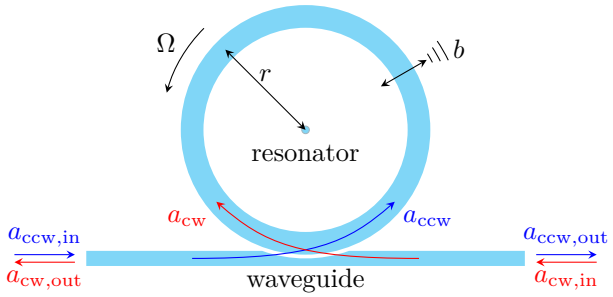

Figure 1. (Color online) Schematic illustration of a spinning optomechanical resonator coupled with a waveguide, where the mechanical mode b is parametrically coupled to two optical cavity modes, i.e., clockwise-propagating mode a_{cw} and counterclockwise-propagating mode a_{ccw}.

In order to make the driving terms time-independent in the Hamiltonian of Equation (1), the unitary transformation $U = \exp\left[-\mathrm{i}\omega_{\mathrm{L}}(a_{\mathrm{cw}}^{\dagger}a_{\mathrm{cw}} + a_{\mathrm{ccw}}^{\dagger}a_{\mathrm{ccw}})t\right]$ is applied to generate a new Hamiltonian $H_{\mathrm{rot}} = U^{\dagger}HU - \mathrm{i}U^{\dagger}H\partial U/\partial t$ of the form

$$\begin{aligned} H_{\mathrm{rot}} = {} & (\Delta + \Delta_{\mathrm{F}})a_{\mathrm{cw}}^{\dagger}a_{\mathrm{cw}} + (\Delta - \Delta_{\mathrm{F}})a_{\mathrm{ccw}}^{\dagger}a_{\mathrm{ccw}} + \omega_{\mathrm{m}}b^{\dagger}b \\ & - g(b + b^{\dagger})(a_{\mathrm{cw}}^{\dagger}a_{\mathrm{cw}} + a_{\mathrm{ccw}}^{\dagger}a_{\mathrm{ccw}}) \\ & + \alpha_{\mathrm{L}}(a_{\mathrm{ccw}} + a_{\mathrm{ccw}}^{\dagger}), \end{aligned} \tag{3}$$

where $\Delta = \omega_{\mathrm{c}} - \omega_{\mathrm{L}}$ is the detuning between resonator and laser. According to the Heisenberg–Langevin approach [60,61], the evolution of the optomechanical system can be described by the set of quantum Langevin equations

$$\begin{aligned} \dot{a}_{\mathrm{cw}} = {} & -[\mathrm{i}(\Delta + \Delta_{\mathrm{F}}) + (\kappa_0 + \kappa)/2]a_{\mathrm{cw}} \\ & + \mathrm{i}g(b + b^{\dagger})a_{\mathrm{cw}} + \sqrt{\kappa}a_{\mathrm{cw,in}}, \end{aligned} \tag{4a}$$

$$\begin{aligned} \dot{a}_{\mathrm{ccw}} = {} & -[\mathrm{i}(\Delta - \Delta_{\mathrm{F}}) + (\kappa_0 + \kappa)/2]a_{\mathrm{ccw}} \\ & + \mathrm{i}g(b + b^{\dagger})a_{\mathrm{ccw}} - \mathrm{i}\alpha_{\mathrm{L}} + \sqrt{\kappa}a_{\mathrm{ccw,in}}, \end{aligned} \tag{4b}$$

$$\begin{aligned} \dot{b} = {} & -(\mathrm{i}\omega_m + \gamma/2)b + \mathrm{i}g\left(a_{\mathrm{cw}}^{\dagger}a_{\mathrm{cw}} + a_{\mathrm{ccw}}^{\dagger}a_{\mathrm{ccw}}\right) \\ & + \sqrt{\gamma}b_{\mathrm{in}}, \end{aligned} \tag{4c}$$

where κ and κ_0 indicate severally the input coupling decay rate and the intrinsic decay rate of the resonator, γ stands for the dissipation rate of the mechanical mode, $a_{\eta,\mathrm{in}}$ ($a_{\eta,\mathrm{out}}$) denotes the input (out) field operator for the mode η, and b_{in} is the thermal noise operator for the mechanical bath. Then, we split each of the system operators $a_{\mathrm{cw/ccw}}$ and b into the steady state value and the fluctuation part, i.e., $a_\eta \to \alpha_\eta + a_\eta$, and $b \to \beta + b$. From Equation (4), equations of motions for the expectation value of the operators are

$$\dot{\alpha}_{\mathrm{cw}} = -\left[\mathrm{i}(\tilde{\Delta} + \Delta_{\mathrm{F}}) + \tilde{\kappa}/2\right]\alpha_{\mathrm{cw}}, \tag{5a}$$

$$\dot{\alpha}_{\mathrm{ccw}} = -\left[\mathrm{i}(\tilde{\Delta} - \Delta_{\mathrm{F}}) + \tilde{\kappa}/2\right]\alpha_{\mathrm{ccw}} - \mathrm{i}\alpha_{\mathrm{L}}, \tag{5b}$$

$$\dot{\beta} = -(\mathrm{i}\omega_m + \gamma/2)\beta + \mathrm{i}g\left(|\alpha_{\mathrm{cw}}|^2 + |\alpha_{\mathrm{ccw}}|^2\right), \tag{5c}$$

where $\tilde{\Delta} = \Delta - g(\beta + \beta^*)$ and $\tilde{\kappa} = \kappa + \kappa_0$. The steady state solutions of Equation (5) are obtained

$$\alpha_{\mathrm{cw}} = 0, \tag{6a}$$

$$\alpha_{\mathrm{ccw}} = \frac{-\mathrm{i}\alpha_{\mathrm{L}}}{\mathrm{i}(\tilde{\Delta} - \Delta_{\mathrm{F}}) + \tilde{\kappa}/2}, \tag{6b}$$

$$\beta = \frac{\mathrm{i}g\left(|\alpha_{\mathrm{cw}}|^2 + |\alpha_{\mathrm{ccw}}|^2\right)}{\mathrm{i}\omega_m + \gamma/2} \tag{6c}$$

by simply taking $\dot{\alpha}_{\mathrm{cw/ccw}} = 0, \dot{\beta} = 0$. When the driving field is strong enough, the high-order small terms in Equation (4) can be neglected. Then, the fluctuations of the system operators are given by

$$\dot{a}_{\mathrm{cw}} = -\left[\mathrm{i}\left(\tilde{\Delta} + \Delta_{\mathrm{F}}\right) + \tilde{\kappa}/2\right]a_{\mathrm{cw}} + \sqrt{\kappa}a_{\mathrm{cw,in}}, \tag{7a}$$

$$\begin{aligned} \dot{a}_{\mathrm{ccw}} = {} & -\left[\mathrm{i}\left(\tilde{\Delta} - \Delta_{\mathrm{F}}\right) + \tilde{\kappa}/2\right]a_{\mathrm{ccw}} + \mathrm{i}G_{\mathrm{ccw}}(b + b^{\dagger}) \\ & + \sqrt{\kappa}a_{\mathrm{ccw,in}}, \end{aligned} \tag{7b}$$

$$\dot{b} = -(\mathrm{i}\omega_m + \gamma/2)b + \mathrm{i}G_{\mathrm{ccw}}\left(a_{\mathrm{ccw}}^{\dagger} + a_{\mathrm{ccw}}\right) + \sqrt{\gamma}b_{\mathrm{in}}. \tag{7c}$$

Here, the combination $G_{\mathrm{ccw}} = g\alpha_{\mathrm{ccw}}$ is referred to the effective optomechanical coupling strength. Without loss of generality, we now assume α_{ccw} is a real value. Thus, the linearized Hamiltonian obtained by the standard linearization procedure [62] reads

$$\begin{aligned} H_{\mathrm{lin}} = {} & (\tilde{\Delta} + \Delta_{\mathrm{F}}) a_{\mathrm{cw}}^{\dagger} a_{\mathrm{cw}} + (\tilde{\Delta} - \Delta_{\mathrm{F}}) a_{\mathrm{ccw}}^{\dagger} a_{\mathrm{ccw}} \\ & + \omega_{\mathrm{m}} b^{\dagger} b - G_{\mathrm{ccw}} \left(a_{\mathrm{ccw}}^{\dagger} + a_{\mathrm{ccw}} \right) (b + b^{\dagger}). \end{aligned} \tag{8}$$

The Hamiltonian, in the interaction picture, is rewritten as

$$\begin{aligned} H_{\mathrm{int}} = {} & -G_{\mathrm{ccw}} \Big\{ \left[a_{\mathrm{ccw}}^{\dagger} b \mathrm{e}^{\mathrm{i}(\tilde{\Delta} - \Delta_{\mathrm{F}} - \omega_{\mathrm{m}})t} + \mathrm{H.c.} \right] \\ & + \left[a_{\mathrm{ccw}}^{\dagger} b^{\dagger} \mathrm{e}^{\mathrm{i}(\tilde{\Delta} - \Delta_{\mathrm{F}} + \omega_{\mathrm{m}})t} + \mathrm{H.c.} \right] \Big\}. \end{aligned} \tag{9}$$

Thereby, in the case of $\tilde{\Delta} - \Delta_{\mathrm{F}} \approx \omega_{\mathrm{m}}$ and rotating-wave approximation, the Hamiltonian of Equation (8) reduces to

$$\begin{aligned} H_{\mathrm{lin}}^{\mathrm{eff}} = {} & (\tilde{\Delta} + \Delta_{\mathrm{F}}) a_{\mathrm{cw}}^{\dagger} a_{\mathrm{cw}} + (\tilde{\Delta} - \Delta_{\mathrm{F}}) a_{\mathrm{ccw}}^{\dagger} a_{\mathrm{ccw}} \\ & + \omega_{\mathrm{m}} b^{\dagger} b - G_{\mathrm{ccw}} \left(a_{\mathrm{ccw}}^{\dagger} b + a_{\mathrm{ccw}} b^{\dagger} \right). \end{aligned} \tag{10}$$

Correspondingly, Equation (7) is simplified to

$$\dot{a}_{\mathrm{cw}} = -\left[\mathrm{i}(\tilde{\Delta} + \Delta_{\mathrm{F}}) + \tilde{\kappa}/2 \right] a_{\mathrm{cw}} + \sqrt{\kappa} a_{\mathrm{cw,in}}, \tag{11a}$$

$$\begin{aligned} \dot{a}_{\mathrm{ccw}} = {} & -\left[\mathrm{i}(\tilde{\Delta} - \Delta_{\mathrm{F}}) + \tilde{\kappa}/2 \right] a_{\mathrm{ccw}} + \mathrm{i} G_{\mathrm{ccw}} b \\ & + \sqrt{\kappa} a_{\mathrm{ccw,in}}, \end{aligned} \tag{11b}$$

$$\dot{b} = -(\mathrm{i}\omega_m + \gamma/2) b + \mathrm{i} G_{\mathrm{ccw}} a_{\mathrm{ccw}} + \sqrt{\gamma} b_{\mathrm{in}}. \tag{11c}$$

3. Implementation of Steering Nonreciprocity

Following the approach of [11] where the resonator is static, we extend it to solve the spinning resonator system.

3.1. Fourier Space

Define the Fourier components of the operator by

$$o(t) = \frac{1}{\sqrt{2\pi}} \int_{-\infty}^{\infty} \mathrm{e}^{-\mathrm{i}\omega t} o(\omega) \, \mathrm{d}\omega. \tag{12}$$

The equations of motion for the fluctuations in the Fourier space are given by

$$-\mathrm{i}\omega a_{\mathrm{cw}} = -\left[\mathrm{i}(\tilde{\Delta} + \Delta_{\mathrm{F}}) + \tilde{\kappa}/2 \right] a_{\mathrm{cw}} + \sqrt{\kappa} a_{\mathrm{cw,in}}, \tag{13a}$$

$$\begin{aligned} -\mathrm{i}\omega a_{\mathrm{ccw}} = {} & -\left[\mathrm{i}(\tilde{\Delta} - \Delta_{\mathrm{F}}) + \tilde{\kappa}/2 \right] a_{\mathrm{ccw}} + \mathrm{i} G_{\mathrm{ccw}} b \\ & + \sqrt{\kappa} a_{\mathrm{ccw,in}}, \end{aligned} \tag{13b}$$

$$-\mathrm{i}\omega b = -(\mathrm{i}\omega_m + \gamma/2) b + \mathrm{i} G_{\mathrm{ccw}} a_{\mathrm{ccw}} + \sqrt{\gamma} b_{\mathrm{in}}. \tag{13c}$$

The solutions of Equation (13) in the frequency space can be expressed as

$$a_{\mathrm{cw}}(\omega) = \frac{\sqrt{\kappa} a_{\mathrm{cw,in}}(\omega)}{\frac{\tilde{\kappa}}{2} - \mathrm{i}[\omega - (\tilde{\Delta} + \Delta_{\mathrm{F}})]}, \tag{14a}$$

$$a_{\mathrm{ccw}}(\omega) = \frac{\sqrt{\kappa} a_{\mathrm{ccw,in}}(\omega) + \mathrm{i} G_{\mathrm{ccw}} b(\omega)}{\frac{\tilde{\kappa}}{2} - \mathrm{i}[\omega - (\tilde{\Delta} - \Delta_{\mathrm{F}})]}, \tag{14b}$$

$$b(\omega) = \frac{\mathrm{i} G_{\mathrm{ccw}} a_{\mathrm{ccw}}(\omega) + \sqrt{\gamma} b_{\mathrm{in}}(\omega)}{\frac{\gamma}{2} - \mathrm{i}(\omega - \omega_{\mathrm{m}})}. \tag{14c}$$

In the case that the vacuum noise operator $b_{\mathrm{in}}(\omega)$ of the mechanical mode is ignored, by inserting Equations (14c) into (14b), the following expression is gained

$$a_{\mathrm{ccw}}(\omega) = \frac{\sqrt{\kappa}a_{\mathrm{ccw,in}}(\omega)}{\frac{\tilde{\kappa}}{2} - \mathrm{i}[\omega - (\tilde{\Delta} - \Delta_{\mathrm{F}})] + \frac{G_{\mathrm{ccw}}^2}{\frac{\gamma}{2} - \mathrm{i}(\omega - \omega_{\mathrm{m}})}}. \tag{15}$$

Based on the input–output theory [61,63,64]

$$a_{\mathrm{cw/ccw,out}}(\omega) + a_{\mathrm{cw/ccw,in}}(\omega) = \sqrt{\kappa}a_{\mathrm{cw/ccw}}(\omega), \tag{16}$$

the output fields are acquired

$$a_{\mathrm{cw,out}}(\omega) = T_{\mathrm{cw}}(\omega)a_{\mathrm{cw,in}}(\omega), \tag{17a}$$
$$a_{\mathrm{ccw,out}}(\omega) = T_{\mathrm{ccw}}(\omega)a_{\mathrm{ccw,in}}(\omega) \tag{17b}$$

with the transmission amplitudes

$$T_{\mathrm{cw}}(\omega) = -1 + \frac{\kappa}{\frac{\tilde{\kappa}}{2} - \mathrm{i}[\omega - (\tilde{\Delta} + \Delta_{\mathrm{F}})]}, \tag{18a}$$
$$T_{\mathrm{ccw}}(\omega) = -1 + \frac{\kappa}{\frac{\tilde{\kappa}}{2} - \mathrm{i}[\omega - (\tilde{\Delta} - \Delta_{\mathrm{F}})] + \frac{G_{\mathrm{ccw}}^2}{\frac{\gamma}{2} - \mathrm{i}(\omega - \omega_{\mathrm{m}})}}. \tag{18b}$$

3.2. Optomechanically Induced Nonreciprocity

The square $|T_{\mathrm{cw/ccw}}|^2$ of the amplitude gives the probability of transmission for the considered optomechanical system. Note that $\tilde{\kappa} = \kappa + \kappa_0$. Depending on the decay rate, three main different regimes can be distinguished [62]. For the overcoupled situation $\kappa_0 \ll \kappa$, $|T_{\mathrm{cw/ccw}}|^2 \approx 1$, the transmissions behave almost the same in both directions. For the undercoupled condition $\kappa_0 \gg \kappa$, it is related to cavity losses dominated by intrinsic losses, which are generally considered unfavorable due to an effective loss of information. For the critical coupling case $\kappa_0 = \kappa$, the transmission amplitudes are

$$T_{\mathrm{cw}} = \frac{\mathrm{i}(\delta - \Delta_{\mathrm{F}})}{\kappa - \mathrm{i}(\delta - \Delta_{\mathrm{F}})}, \tag{19a}$$
$$T_{\mathrm{ccw}} = \frac{(\delta + \Delta_{\mathrm{F}})^2 - G_{\mathrm{ccw}}^2}{G_{\mathrm{ccw}}^2 - (\delta + \Delta_{\mathrm{F}})^2 - \mathrm{i}\kappa(\delta + \Delta_{\mathrm{F}})}, \tag{19b}$$

where $\delta = \omega - \tilde{\Delta}$, and it has been assumed that the mechanical decay rate γ is small enough to be ignored with insignificant impact on the system.

Figure 2 shows the transmission probability $|T_{\mathrm{cw,ccw}}|^2$ of the optical input field as a function of detuning δ for various values of the Fizeau shift Δ_{F}. When $\Delta_{\mathrm{F}} = 0$, the curves exhibit the nonreciprocal transmissions at $\delta = 0$, where the cw input is almost absorbed by the cavity and the ccw input transmits with the probability close to unity (see Figure 2b). However, the transmission probabilities are reversed at $\delta = 0$ for cw and ccw input fields when the cavity acquires a frequency shift Δ_{F} for the spinning resonator (see Figure 2a,c). Similarly, the system also exhibits nonreciprocity at other detuning values, as illustrated in Figure 2: (a) $\delta = -\Delta_{\mathrm{F}} - G_{\mathrm{ccw}}$ and $\delta = \Delta_{\mathrm{F}}$ when $\Delta_{\mathrm{F}} = G_{\mathrm{ccw}}$, (b) $\delta = \pm G_{\mathrm{ccw}}$ when $\Delta_{\mathrm{F}} = 0$, (c) $\delta = -G_{\mathrm{ccw}}$ and $\delta = -\Delta_{\mathrm{F}} + G_{\mathrm{ccw}}$ when $\Delta_{\mathrm{F}} = -G_{\mathrm{ccw}}$. In order to observe a clear reversion of the transmission amplitudes for cw and ccw modes, the frequency shift Δ_F should be greater than the cavity decay rate κ. To show this clearly, transmission probabilities for $|\Delta_F| = 0.5\kappa$ are plotted in the right panel of Figure 2. At $\delta = 0$, Figure 2d,f display that the transmission probabilities for ccw and cw modes are zero and well below one, respectively, which imply the breakdown of nonreciprocity.

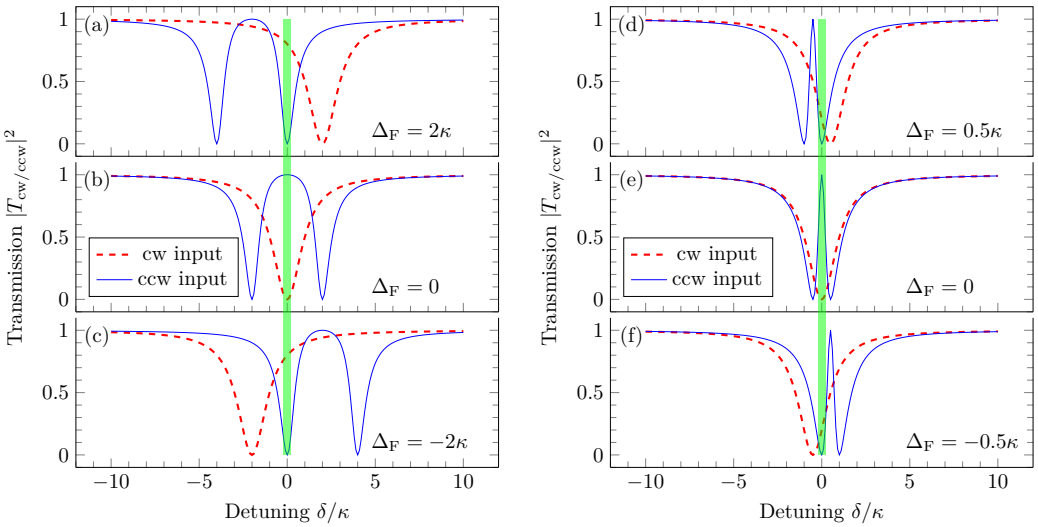

Figure 2. (Color online) Transmission probability $|T_{cw,ccw}|^2$ of the optical input field versus the detuning δ for various values of the Fizeau shift Δ_F. The dashed (red) curve is the transmission probability for the cw input, while the solid (blue) line is the transmission probability for the ccw input. Parameter in (**a**–**c**): $G_{ccw} = 2\kappa$; (**d**–**f**): $G_{ccw} = 0.5\kappa$. Other parameters are taken as $\kappa_0 = \kappa, \gamma = 0$.

In addition, Figure 3 plots $|T_{cw,ccw}|^2$ as a function of the Fizeau shift Δ_F for detuning $\delta = 0$. Clearly, the system performs a function similar to a controllable optical diode at $\delta = 0$. When the resonator is static, i.e., $\Delta_F = 0$, counterclockwise-incident light passes unalterably, but clockwise-incident light is completely absorbed. When the resonator is rotated to introduce the Fizeau shift $\Delta_F = \pm G_{ccw} = \pm 2\kappa$, light passes almost unaltered in the clockwise direction, but is almost completely absorbed in the counterclockwise direction. Thus, this rotation system implements a controllable optical diode.

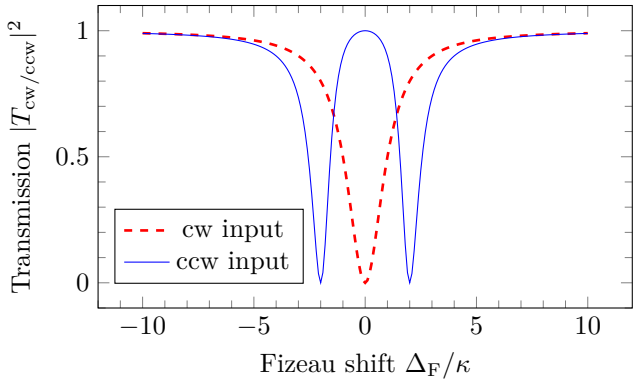

Figure 3. (Color online) Transmission probability $|T_{cw,ccw}|^2$ of the optical input field versus the Fizeau shift Δ_F for detuning $\delta = 0$. The dashed (red) curve denotes the transmission probability for the cw input, while the solid (blue) line denotes the transmission probability for the ccw input. Here, $\delta = 0$, other parameters are the same as those in Figure 2.

3.3. Nonreciprocity without Optomechanical Coupling

It is natural to ask whether it is possible to regulate the nonreciprocal transmission if there does not exist optomechanical coupling, i.e., $g = 0$. Now, the Hamiltonian is simply

$$H = (\omega_c + \Delta_F)a_{cw}^\dagger a_{cw} + (\omega_c - \Delta_F)a_{ccw}^\dagger a_{ccw}. \tag{20}$$

In a similar manner as above, the following form of the transmission amplitudes is obtained

$$T_{\mathrm{cw}} = \frac{\mathrm{i}(\delta_{\mathrm{c}} - \Delta_{\mathrm{F}})}{\kappa - \mathrm{i}(\delta_{\mathrm{c}} - \Delta_{\mathrm{F}})}, \tag{21a}$$

$$T_{\mathrm{ccw}} = \frac{\mathrm{i}(\delta_{\mathrm{c}} + \Delta_{\mathrm{F}})}{\kappa - \mathrm{i}(\delta_{\mathrm{c}} + \Delta_{\mathrm{F}})} \tag{21b}$$

in the critical coupling case of $\kappa_0 = \kappa$, where $\delta_{\mathrm{c}} = \omega - \omega_{\mathrm{c}}$.

According to Equation (21), the transmission probability $|T_{\mathrm{cw,ccw}}|^2$ as a function of detuning δ_{c} for various values of the Fizeau shift Δ_{F} is displayed in Figure 4. Notice that the curves overlap at $\Delta_{\mathrm{F}} = 0$ since the system is symmetrical, as shown in Figure 4b,e, which means no nonreciprocity. When the resonator is rotated, the frequencies of cw and ccw fields will separately gain a Fizeau shift Δ_{F} but with different signs. For a sufficiently large Δ_{F}, if the cw (ccw) input field is tuned to resonance with the cavity, the light from the opposite direction will be strongly detuned, which makes only one of the input lights pass through the system. Hence, even if there is no optomechanical coupling, the system presents nonreciprocal characteristics at $\delta_{\mathrm{c}} = \pm\Delta_{\mathrm{F}}$ as seen from Figure 4a,c. Obviously, unlike the optomechanically induced case, the system without optomechanical coupling does not exhibit nonreciprocal transmission at $\delta_{\mathrm{c}} = 0$. However, if the detuning δ_{c} is tuned to $\pm\Delta_{\mathrm{F}}$, the system still behaves as an optical diode. We also plot the transmission probabilities with $\Delta_F = 0.5\kappa$ in Figure 4d,f, where it can be seen that the nonreciprocal characteristics vanish. To observe the nonreciprocal characteristics for cw and ccw modes, the frequency shift Δ_F must be larger than the cavity linewidth κ. This is similar to the case with optomechanical coupling.

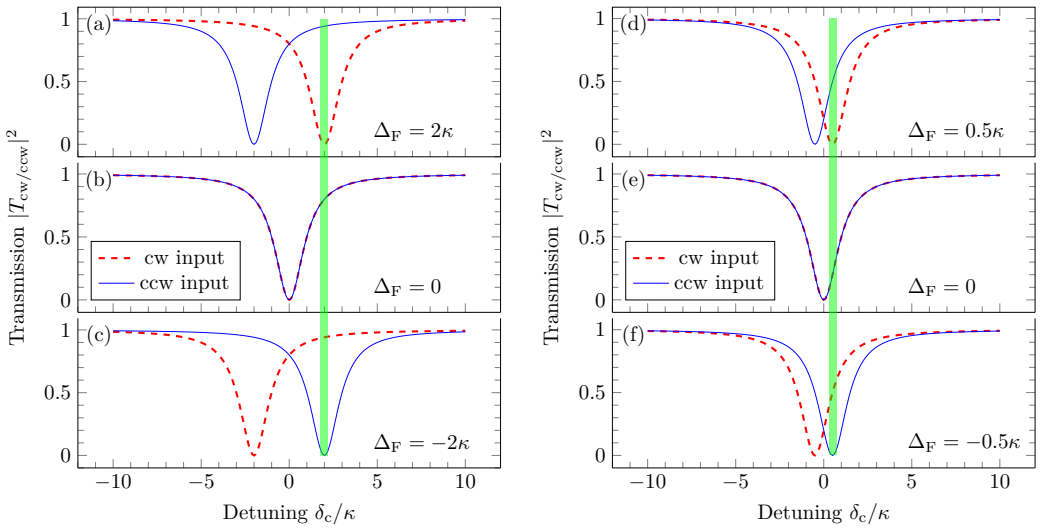

Figure 4. (Color online) Transmission probability $|T_{\mathrm{cw,ccw}}|^2$ of the optical input field versus the detuning δ_{c} for various values of the Fizeau shift Δ_{F}. The dashed (red) curve denotes the transmission probability for the cw input, while the solid (blue) line denotes the transmission probability for the ccw input. Parameter in (**a**–**c**): $G_{\mathrm{ccw}} = 2\kappa$; (**d**–**f**): $G_{\mathrm{ccw}} = 0.5\kappa$. Other parameters are the same as those in Figure 2.

4. Discussion and Conclusions

Finally, we analyze the feasibility of the scheme according to the recent experimental parameters realized in [14,15,65]. Based on these systems, the frequency of a mechanical mode can reach $\omega_{\mathrm{m}}/(2\pi) = 78\,\mathrm{MHz}$, the effective optomechanical coupling strength has been enhanced up to $G_{\mathrm{ccw}}/(2\pi) = 11.4\,\mathrm{MHz}$, and the resonator decay rate is $\kappa/(2\pi) = 7.1\,\mathrm{MHz}$. So far, the Fizeau shift about 24 MHz has been achieved for the angular velocity $\Omega = 6.6\,\mathrm{kHz}$ in the spinning resonator [37]. It is worth noting that the

key parameter $|\Delta_F| > \kappa$ meets the requirement of our scheme, which provides a large dynamic adjustment range for the transmission probability. If the experimental parameters of a stationary resonator can be obtained in a rotating cavity under critical coupling, it is possible to regulate nonreciprocity with a spinning resonator under currently available experimental conditions.

In summary, we have presented an approach to steer nonreciprocity by exploiting a spinning resonator. The spinning resonator acting as a controller can revise the transmission probabilities of incident lights in two opposite directions of the waveguide. Our scheme is an extension of the previous proposal [11], where the nonreciprocity of the light is proposed by using only the optomechanical coupling. We show here that such a nonreciprocity can be steered by exploiting the Sagnac–Fizeau effect. We also show that the regulable nonreciprocity exists even without the optomechanical coupling. This is different from recent work [40], which focused on tuning the properties of optomechanically induced transparency in a spinning resonator. The present scheme may be useful for realizing controllable nonreciprocal devices.

Author Contributions: Conceptualization, X.S. and H.X.; methodology, X.S. and H.X.; validation, X.S., H.X. and G.L.; formal analysis, X.S. and H.X.; investigation, X.S. and H.X.; resources, X.S. and X.L.; writing—original draft preparation, X.S.; writing—review and editing, H.X., G.L. and X.L.; visualization, X.S. All authors have read and agreed to the published version of the manuscript.

Funding: This research was funded by the National Natural Science Foundation of China under Grants No. 12074067, No. 12174054, and No. 11674059, the Natural Science Foundation of Fujian Province of China under Grants No. 2020J01191 and No. 2019J01431.

Institutional Review Board Statement: Not applicable.

Informed Consent Statement: Not applicable.

Data Availability Statement: Not applicable.

Conflicts of Interest: The authors declare no conflicts of interest.

References

1. Caloz, C.; Alù, A.; Tretyakov, S.; Sounas, D.; Achouri, K.; Deck-Léger, Z.L. Electromagnetic Nonreciprocity. *Phys. Rev. Appl.* **2018**, *10*, 047001. [CrossRef]
2. Verhagen, E.; Alù, A. Optomechanical nonreciprocity. *Nat. Phys.* **2017**, *13*, 922–924. [CrossRef]
3. Rosario Hamann, A.; Müller, C.; Jerger, M.; Zanner, M.; Combes, J.; Pletyukhov, M.; Weides, M.; Stace, T.M.; Fedorov, A. Nonreciprocity Realized with Quantum Nonlinearity. *Phys. Rev. Lett.* **2018**, *121*, 123601. [CrossRef]
4. Yu, Z.; Fan, S. Complete optical isolation created by indirect interband photonic transitions. *Nat. Photonics* **2009**, *3*, 91–94. [CrossRef]
5. Lira, H.; Yu, Z.; Fan, S.; Lipson, M. Electrically Driven Nonreciprocity Induced by Interband Photonic Transition on a Silicon Chip. *Phys. Rev. Lett.* **2012**, *109*, 033901. [CrossRef]
6. Sounas, D.L.; Alù, A. Non-reciprocal photonics based on time modulation. *Nat. Photonics* **2017**, *11*, 774–783. [CrossRef]
7. Sohn, D.B.; Kim, S.; Bahl, G. Time-reversal symmetry breaking with acoustic pumping of nanophotonic circuits. *Nat. Photonics* **2018**, *12*, 91–97. [CrossRef]
8. Fang, K.; Yu, Z.; Fan, S. Realizing effective magnetic field for photons by controlling the phase of dynamic modulation. *Nat. Photonics* **2012**, *6*, 782–787. [CrossRef]
9. Tzuang, L.D.; Fang, K.; Nussenzveig, P.; Fan, S.; Lipson, M. Non-reciprocal phase shift induced by an effective magnetic flux for light. *Nat. Photonics* **2014**, *8*, 701–705. [CrossRef]
10. Fang, K.; Luo, J.; Metelmann, A.; Matheny, M.H.; Marquardt, F.; Clerk, A.A.; Painter, O. Generalized non-reciprocity in an optomechanical circuit via synthetic magnetism and reservoir engineering. *Nat. Phys.* **2017**, *13*, 465–471. [CrossRef]
11. Hafezi, M.; Rabl, P. Optomechanically induced non-reciprocity in microring resonators. *Opt. Express* **2012**, *20*, 7672–7684. [CrossRef] [PubMed]
12. Kim, J.; Kuzyk, M.C.; Han, K.; Wang, H.; Bahl, G. Non-reciprocal Brillouin scattering induced transparency. *Nat. Phys.* **2015**, *11*, 275–280. [CrossRef]
13. Dong, C.H.; Shen, Z.; Zou, C.L.; Zhang, Y.L.; Fu, W.; Guo, G.C. Brillouin-scattering-induced transparency and non-reciprocal light storage. *Nat. Commun.* **2015**, *6*, 6193. [CrossRef] [PubMed]
14. Shen, Z.; Zhang, Y.L.; Chen, Y.; Zou, C.L.; Xiao, Y.F.; Zou, X.B.; Sun, F.W.; Guo, G.C.; Dong, C.H. Experimental realization of optomechanically induced non-reciprocity. *Nat. Photonics* **2016**, *10*, 657. [CrossRef]

15. Shen, Z.; Zhang, Y.L.; Chen, Y.; Sun, F.W.; Zou, X.B.; Guo, G.C.; Zou, C.L.; Dong, C.H. Reconfigurable optomechanical circulator and directional amplifier. *Nat. Commun.* **2018**, *9*, 1797. [CrossRef]
16. Ruesink, F.; Miri, M.A.; Alù, A.; Verhagen, E. Nonreciprocity and magnetic-free isolation based on optomechanical interactions. *Nat. Commun.* **2016**, *7*, 13662. [CrossRef]
17. Bernier, N.R.; Tóth, L.D.; Koottandavida, A.; Ioannou, M.A.; Malz, D.; Nunnenkamp, A.; Feofanov, A.K.; Kippenberg, T.J. Nonreciprocal reconfigurable microwave optomechanical circuit. *Nat. Commun.* **2017**, *8*, 604. [CrossRef]
18. Peterson, G.A.; Lecocq, F.; Cicak, K.; Simmonds, R.W.; Aumentado, J.; Teufel, J.D. Demonstration of Efficient Nonreciprocity in a Microwave Optomechanical Circuit. *Phys. Rev. X* **2017**, *7*, 031001. [CrossRef]
19. Barzanjeh, S.; Wulf, M.; Peruzzo, M.; Kalaee, M.; Dieterle, P.B.; Painter, O.; Fink, J.M. Mechanical on-chip microwave circulator. *Nat. Commun.* **2017**, *8*, 953. [CrossRef]
20. Miri, M.A.; Ruesink, F.; Verhagen, E.; Alù, A. Optical Nonreciprocity Based on Optomechanical Coupling. *Phys. Rev. Appl.* **2017**, *7*, 064014. [CrossRef]
21. Ruesink, F.; Mathew, J.P.; Miri, M.A.; Alù, A.; Verhagen, E. Optical circulation in a multimode optomechanical resonator. *Nat. Commun.* **2018**, *9*, 1798. [CrossRef] [PubMed]
22. Kittlaus, E.A.; Otterstrom, N.T.; Kharel, P.; Gertler, S.; Rakich, P.T. Non-reciprocal interband Brillouin modulation. *Nat. Photonics* **2018**, *12*, 613–619. [CrossRef]
23. Ren, L.; Xu, X.; Zhu, S.; Shi, L.; Zhang, X. Experimental Realization of on-Chip Nonreciprocal Transmission by Using the Mechanical Kerr Effect. *ACS Photonics* **2020**, *7*, 2995–3002. [CrossRef]
24. Peng, B.; Özdemir, Ş.K.; Lei, F.; Monifi, F.; Gianfreda, M.; Long, G.L.; Fan, S.; Nori, F.; Bender, C.M.; Yang, L. Parity–time-symmetric whispering-gallery microcavities. *Nat. Phys.* **2014**, *10*, 394–398. [CrossRef]
25. Chang, L.; Jiang, X.; Hua, S.; Yang, C.; Wen, J.; Jiang, L.; Li, G.; Wang, G.; Xiao, M. Parity–time symmetry and variable optical isolation in active–passive-coupled microresonators. *Nat. Photonics* **2014**, *8*, 524–529. [CrossRef]
26. Jin, B.; Argyropoulos, C. Nonreciprocal Transmission in Nonlinear PT-Symmetric Metamaterials Using Epsilon-Near-Zero Media Doped with Defects. *Adv. Opt. Mater.* **2019**, *7*, 1901083. [CrossRef]
27. Shao, L.; Mao, W.; Maity, S.; Sinclair, N.; Hu, Y.; Yang, L.; Lončar, M. Non-reciprocal transmission of microwave acoustic waves in nonlinear parity–time symmetric resonators. *Nat. Electron.* **2020**, *3*, 267–272. [CrossRef]
28. Cao, Q.T.; Wang, H.; Dong, C.H.; Jing, H.; Liu, R.S.; Chen, X.; Ge, L.; Gong, Q.; Xiao, Y.F. Experimental Demonstration of Spontaneous Chirality in a Nonlinear Microresonator. *Phys. Rev. Lett.* **2017**, *118*, 033901. [CrossRef]
29. Bino, L.D.; Silver, J.M.; Woodley, M.T.M.; Stebbings, S.L.; Zhao, X.; Del'Haye, P. Microresonator isolators and circulators based on the intrinsic nonreciprocity of the Kerr effect. *Optica* **2018**, *5*, 279–282. [CrossRef]
30. Zhang, S.; Hu, Y.; Lin, G.; Niu, Y.; Xia, K.; Gong, J.; Gong, S. Thermal-motion-induced non-reciprocal quantum optical system. *Nat. Photonics* **2018**, *12*, 744–748. [CrossRef]
31. Xia, K.; Nori, F.; Xiao, M. Cavity-Free Optical Isolators and Circulators Using a Chiral Cross-Kerr Nonlinearity. *Phys. Rev. Lett.* **2018**, *121*, 203602. [CrossRef] [PubMed]
32. Tang, L.; Tang, J.; Zhang, W.; Lu, G.; Zhang, H.; Zhang, Y.; Xia, K.; Xiao, M. On-chip chiral single-photon interface: Isolation and unidirectional emission. *Phys. Rev. A* **2019**, *99*, 043833. [CrossRef]
33. Yang, P.; Xia, X.; He, H.; Li, S.; Han, X.; Zhang, P.; Li, G.; Zhang, P.; Xu, J.; Yang, Y.; et al. Realization of Nonlinear Optical Nonreciprocity on a Few-Photon Level Based on Atoms Strongly Coupled to an Asymmetric Cavity. *Phys. Rev. Lett.* **2019**, *123*, 233604. [CrossRef] [PubMed]
34. Sohn, D.B.; Örsel, O.E.; Bahl, G. Electrically driven optical isolation through phonon-mediated photonic Autler–Townes splitting. *Nat. Photonics* **2021**, *15*, 822–827. [CrossRef]
35. Tian, H.; Liu, J.; Siddharth, A.; Wang, R.N.; Blésin, T.; He, J.; Kippenberg, T.J.; Bhave, S.A. Magnetic-free silicon nitride integrated optical isolator. *Nat. Photonics* **2021**, *15*, 828–836. [CrossRef]
36. Tang, L.; Tang, J.; Chen, M.; Nori, F.; Xiao, M.; Xia, K. Quantum Squeezing Induced Optical Nonreciprocity. *Phys. Rev. Lett.* **2022**, *128*, 083604. [CrossRef] [PubMed]
37. Maayani, S.; Dahan, R.; Kligerman, Y.; Moses, E.; Hassan, A.U.; Jing, H.; Nori, F.; Christodoulides, D.N.; Carmon, T. Flying couplers above spinning resonators generate irreversible refraction. *Nature* **2018**, *558*, 569–572. [CrossRef]
38. Huang, R.; Miranowicz, A.; Liao, J.Q.; Nori, F.; Jing, H. Nonreciprocal Photon Blockade. *Phys. Rev. Lett.* **2018**, *121*, 153601. [CrossRef]
39. Malykin, G.B. The Sagnac effect: Correct and incorrect explanations. *Physics-Uspekhi* **2000**, *43*, 1229–1252. [CrossRef]
40. Lü, H.; Jiang, Y.; Wang, Y.Z.; Jing, H. Optomechanically induced transparency in a spinning resonator. *Photon. Res.* **2017**, *5*, 367–371. [CrossRef]
41. Mirza, I.M.; Ge, W.; Jing, H. Optical nonreciprocity and slow light in coupled spinning optomechanical resonators. *Opt. Express* **2019**, *27*, 25515–25530. [CrossRef] [PubMed]
42. Li, B.; Özdemir, S.K.; Xu, X.W.; Zhang, L.; Kuang, L.M.; Jing, H. Nonreciprocal optical solitons in a spinning Kerr resonator. *Phys. Rev. A* **2021**, *103*, 053522. [CrossRef]
43. Zhou, N.N.; Zhang, L.Q.; Yu, C.S. Mechanically controllable nonreciprocal transmission and perfect absorption of photons. *Opt. Express* **2022**, *30*, 24431–24442. [CrossRef]
44. Li, B.; Huang, R.; Xu, X.; Miranowicz, A.; Jing, H. Nonreciprocal unconventional photon blockade in a spinning optomechanical system. *Photon. Res.* **2019**, *7*, 630–641. [CrossRef]

45. Jing, Y.W.; Shi, H.Q.; Xu, X.W. Nonreciprocal photon blockade and directional amplification in a spinning resonator coupled to a two-level atom. *Phys. Rev. A* **2021**, *104*, 033707. [CrossRef]
46. Shang, X.; Xie, H.; Lin, X.M. Nonreciprocal photon blockade in a spinning optomechanical resonator. *Laser Phys. Lett.* **2021**, *18*, 115202. [CrossRef]
47. Xue, W.S.; Shen, H.Z.; Yi, X.X. Nonreciprocal conventional photon blockade in driven dissipative atom-cavity. *Opt. Lett.* **2020**, *45*, 4424–4427. [CrossRef]
48. Shen, H.Z.; Wang, Q.; Wang, J.; Yi, X.X. Nonreciprocal unconventional photon blockade in a driven dissipative cavity with parametric amplification. *Phys. Rev. A* **2020**, *101*, 013826. [CrossRef]
49. Yao, X.Y.; Ali, H.; Li, F.L.; Li, P.B. Nonreciprocal Phonon Blockade in a Spinning Acoustic Ring Cavity Coupled to a Two-Level System. *Phys. Rev. Appl.* **2022**, *17*, 054004. [CrossRef]
50. Jiang, Y.; Maayani, S.; Carmon, T.; Nori, F.; Jing, H. Nonreciprocal Phonon Laser. *Phys. Rev. Appl.* **2018**, *10*, 064037. [CrossRef]
51. Li, W.A.; Huang, G.Y.; Chen, J.P.; Chen, Y. Nonreciprocal enhancement of optomechanical second-order sidebands in a spinning resonator. *Phys. Rev. A* **2020**, *102*, 033526. [CrossRef]
52. Xu, Y.; Liu, J.Y.; Liu, W.; Xiao, Y.F. Nonreciprocal phonon laser in a spinning microwave magnomechanical system. *Phys. Rev. A* **2021**, *103*, 053501. [CrossRef]
53. Xu, Y.J.; Song, J. Nonreciprocal magnon laser. *Opt. Lett.* **2021**, *46*, 5276–5279. [CrossRef]
54. Jiao, Y.F.; Zhang, S.D.; Zhang, Y.L.; Miranowicz, A.; Kuang, L.M.; Jing, H. Nonreciprocal Optomechanical Entanglement against Backscattering Losses. *Phys. Rev. Lett.* **2020**, *125*, 143605. [CrossRef] [PubMed]
55. Yang, Z.B.; Liu, J.S.; Zhu, A.D.; Liu, H.Y.; Yang, R.C. Nonreciprocal Transmission and Nonreciprocal Entanglement in a Spinning Microwave Magnomechanical System. *Ann. Phys.* **2020**, *532*, 2000196. [CrossRef]
56. Ren, Y.L. Nonreciprocal optical–microwave entanglement in a spinning magnetic resonator. *Opt. Lett.* **2022**, *47*, 1125–1128. [CrossRef] [PubMed]
57. Zhang, D.W.; Zheng, L.L.; You, C.; Hu, C.S.; Wu, Y.; Lü, X.Y. Nonreciprocal chaos in a spinning optomechanical resonator. *Phys. Rev. A* **2021**, *104*, 033522. [CrossRef]
58. Schliesser, A.; Kippenberg, T.J. Cavity Optomechanics with Whispering-Gallery Mode Optical Micro-Resonators. *Adv. At. Mol. Opt. Phys.* **2010**, *58*, 207–323. [CrossRef]
59. Shi, H.; Xiong, Z.; Chen, W.; Xu, J.; Wang, S.; Chen, Y. Gauge-field description of Sagnac frequency shift and mode hybridization in a rotating cavity. *Opt. Express* **2019**, *27*, 28114–28122. [CrossRef]
60. Gardiner, C.; Zoller, P.; Zoller, P. *Quantum Noise: A Handbook of Markovian and Non-Markovian Quantum Stochastic Methods with Applications to Quantum Optics*; Springer: Berlin/Heidelberg, Germany; New York, NY, USA, 2004.
61. Walls, D.F.; Milburn, G.J. *Quantum Optics*; Springer: Berlin/Heidelberg, Germany, 2008. [CrossRef]
62. Aspelmeyer, M.; Kippenberg, T.J.; Marquardt, F. Cavity optomechanics. *Rev. Mod. Phys.* **2014**, *86*, 1391–1452. [CrossRef]
63. Gardiner, C.W.; Collett, M.J. Input and output in damped quantum systems: Quantum stochastic differential equations and the master equation. *Phys. Rev. A* **1985**, *31*, 3761–3774. [CrossRef] [PubMed]
64. Fabre, C.; Pinard, M.; Bourzeix, S.; Heidmann, A.; Giacobino, E.; Reynaud, S. Quantum-noise reduction using a cavity with a movable mirror. *Phys. Rev. A* **1994**, *49*, 1337–1343. [CrossRef] [PubMed]
65. Verhagen, E.; Deléglise, S.; Weis, S.; Schliesser, A.; Kippenberg, T.J. Quantum-coherent coupling of a mechanical oscillator to an optical cavity mode. *Nature* **2012**, *482*, 63–67. [CrossRef] [PubMed]